

Project of Strategic Interest NEXTDATA

D1.1.D: Future elevation-dependent warming on Italian mountains and related database

Prepared by: E. Palazzi
CNR-ISAC, Torino

Contributors:
J. von Hardenberg, S. Terzago, L. Mortarini
CNR-ISAC, Torino

This deliverable is structured into two sections, the first describes the phenomenon which is referred to as Elevation-Dependent Warming (EDW) and the second introduces the database that has been used to assess EDW and its characteristics, with special focus on EDW future projections in the Alpine region.

1. Elevation-Dependent Warming

The average global temperature on Earth has increased of about 1°C since 1880, the time around which the measuring stations started to sufficiently cover enough of the planet to have reliable and homogeneous temperature timeseries. A one-degree temperature increase averaged over the globe is a significant amount mainly for two reasons. One is that it takes a vast amount of additional heat stored in the Earth climate system to warm the oceans, the atmosphere, and the land by that much. The other is that such an averaged amount translates into a temperature increase which can differ a lot from one region to another. Warming is not uniform across the globe indeed. For example, it is generally greater over land than over the oceans. Some land areas, moreover, have warmed more and faster than others or compared to the globally-averaged temperature increase. One generally refers to these areas as climate “hot-spot” regions. Hot-spots, both because they undergo greater warming rates than the rest of the globe and also because the impact of the temperature increase in these regions is amplified, compromising mountain ecosystems and the services which they provide. The enhancement of warming rates with elevation is referred to as elevation-dependent warming, or EDW (Pepin et al., 2015). EDW has important implications for the mass balance of the high-altitude cryosphere leading to consequences for water storage in the various reservoirs and for future water availability, thus impacting on downstream societies.

In recent years, the number of studies that have analysed EDW has increased (see Pepin et al. 2015 for a comprehensive review on this topic). These studies differ in the type of data that have been employed, in the considered mountain ranges, and in the methods of analysis used to identify and quantify EDW.

Causes of EDW

Several mechanisms have been recognized as possible drivers of EDW. A full review of them can be found in Rangwala et al (2012) and in Pepin et al (2015), and references therein. Causes of EDW can be associated with either an elevation-dependent change in key variables such as snow and ice cover, clouds, water vapor amount, aerosols, soil moisture, or an elevation-dependent sensitivity of surface warming to changes in these possible drivers. This already suggests that EDW is a complex phenomenon, complicated by a number of variables which interact with each other, possibly giving rise to feedback mechanisms. All this, together with the limitations inherent in both high-altitude observations and in model simulations over complex regions, makes it very difficult to study EDW and to disentangle its causes.

- *The snow/ice albedo feedback*, illustrated in a simple way in Fig. 1, is among the strongest feedback loops active in the climate system, particularly important in cold mountain regions. In response to a temperature increase, more snow or ice melts thus decreasing the local albedo, allowing for increased absorption of solar radiation and, by consequence, for an enhancement of the initial warming. Since this feedback modulates the surface absorption of incoming solar radiation, it is expected to affect primarily maximum temperatures (daytime temperatures). Nevertheless, it has been found that this feedback also acts in modulating nighttime minimum temperatures, especially when decreases in snow cover are accompanied by increases in soil

moisture. This feedback is most effective at elevations around the annual 0°C isotherm (Pepin and Lundquist, 2008, Palazzi et al., 2017) and it is expected to act predominantly at lower elevations earlier in the cold season while at higher elevations later on.

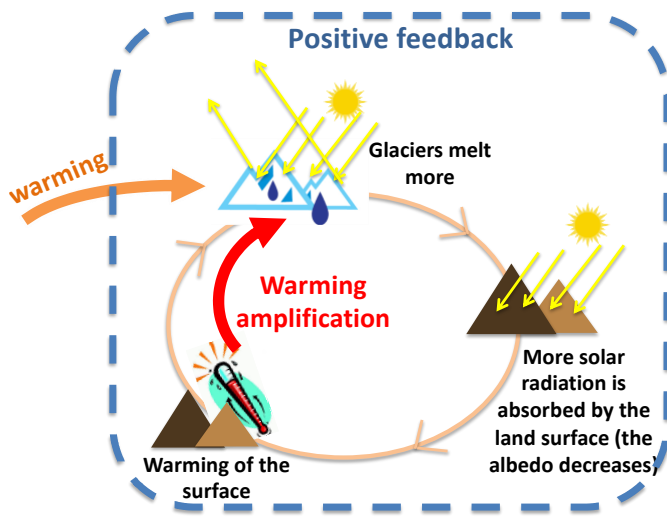


Figure 1. Sketch on how the ice/snow albedo positive feedback works, resulting in an amplification of an initial warming in high-elevation regions.

- *Clouds* are among the most uncertain components of the climate system, affecting both shortwave and longwave radiation. As a consequence, their effect on the climate system is twofold. The clouds which are effective in reflecting shortwave radiation can lead to cooling, while those which absorb and re-emit terrestrial longwave radiation lead to warming. As a consequence, a decrease in cloud cover during the day is expected to enhance the maximum temperature, while a decrease in cloud cover during the night is expected to lower the minimum temperature. For example, observational and model studies conducted over the Tibetan Plateau showed that an increase in cloud cover during the night can lead to EDW in the minimum temperature in this area (Duan and Wu 2006). Quantifying cloud feedbacks still remain challenging and mostly rely on the use of numerical models of the climate system.
- A warmer atmosphere is able to hold more *water vapor*. Water vapor is a powerful greenhouse gas and, as such, it participates in one of the most important feedback loops active in the climate system, the water vapor/greenhouse gas feedback: more water vapour in the atmosphere leads to more warming which leads to more water vapour, and so on and so forth. Increases in surface specific humidity have been suggested to be partly responsible for a rapid increase in surface warming in the Tibetan Plateau (Rangwala et al. 2010) in the late 20th century. This is related to the relationship between the increases in specific humidity and the increases in downward longwave radiation (DLR), which produces a surface warming. Although increases in downward longwave radiation associated with increasing specific humidity occur globally, the sensitivity is non-linear and it is enhanced when the initial humidity is low as is commonly found at high elevations during the cold season.
- *Absorbing aerosols* like black carbon (soot) and dust are additional contributors to warming the climate system. In their review paper, Ramanathan and Carmichael (2008) suggested that black carbon in the Himalayan Mountains arising from

anthropogenic activities might be responsible for half the total warming there during the last decades. Because black carbon both absorbs solar radiation in the troposphere and decreases surface albedo when deposited on snow or ice, it is very difficult to assess its effect on elevation-dependent warming. Depending on the elevation at which black carbon is deposited it could either contribute to enhanced or reduced warming with elevation during the melt season. Similar to black carbon, dust absorbs radiation within the atmosphere and reduces surface albedo when deposited on snow. Similarly to black carbon, however, the impact of dust on elevation-dependent warming will depend on the elevation at which it is deposited.

Difficulties in studying EDW

Even ignoring external forcing factors impinging upon mountains such as land use/cover changes or climate and environmental changes, features like topography, slope, aspect and exposure alone would make the temperatures measured in mountain regions characterized by extreme local-scale variability. All this makes it difficult to study climate processes in the mountains and to understand the mechanisms driving amplified warming rates in high-altitude regions.

The complexity and heterogeneity of mountain environments and climate would require a dense and homogeneous network of ground stations up to the highest altitudes, which is not the situation generally encountered in most mountain areas: the picture provided by all observation-based datasets is, therefore, biased towards the lower elevations. Long-term time series are moreover required to calculate temperature trends and to assess their dependence on elevation, but meteorological stations with at least 20-30 years of records are very few at very high elevations (Pepin et al., 2015). In spite of these limitations, the majority of studies on EDW is based on the analysis of surface station observations, and a few of them are based on estimates of land surface temperature from satellite (e.g., Qin et al. 2009). Most observational studies indicate that warming rates are amplified with elevation, depending on the season, the region of study and the analysed variable (usually either the minimum or maximum daily temperature). There are also studies, however, showing no clear correlation between temperature trends and surface elevation and others depicting more complex relationships. “Mixed” results on EDW are likely dependent on the limitations of the current networks of in situ stations, on the presence of possible non-climatic artifacts associated with changes in measurement practices, on the different methods adopted to homogenize time series and on procedures used to interpolate in situ station data.

The use of climate models, both global and regional, to study EDW allows to overcome some of the inadequacies inherent in all observing systems especially when trying to identify the main mechanisms at work. The output of numerical models, in fact, includes all the variables needed to build a picture of the mechanisms driving EDW, at a given spatial and temporal resolution, and long simulations can be run both to reproduce the past and to study future projections. A majority of model studies on EDW is based on global climate models, in spite of their coarse horizontal resolutions (on average coarser than 120 km; Taylor et al. 2012). Some studies used simulations from a single GCM (e.g., Fyfe and Flato 1999; Liu et al. 2009; Yan et al. 2016), while others analysed the output of several models with different characteristics, such as the latest CMIP5 GCM ensemble (e.g., Rangwala et al. 2013, 2016; Palazzi et al. 2017).

Over the recent decades, global climate models have considerably increased the number of components incorporated within them and the degree of detail in the description of the key climate processes (IPCC 2013). At the same time, global models have been tested at

increasing horizontal resolutions reaching, at least in specific experiments, grid scales that are typically achieved by numerical weather prediction models (e.g., Demory et al. 2014; Davini et al. 2017).

2. EDW projections for the Alpine region and related dataset

The results of one study (Palazzi et al., 2018) which analyses EDW in three different mountain regions (shown in Fig. 2) using high-resolution simulations of one state-of-the-art Global Climate Model are summarized in this section, focusing on one of the analysed regions only, the Greater Alpine Region (GAR). We used EC-Earth (Hazeleger et al. 2010, 2012) climate simulations at five different spatial resolutions, from ~ 125 to ~ 16 km, the coarsest resolution being the one typically used in state-of-the-art global climate model simulations (e.g. in CMIP5), while the finest being the resolution typically used for numerical weather predictions. One aim of this study, in fact, was to investigate the impact of the model spatial resolution on the representation of EDW and its driving mechanisms.

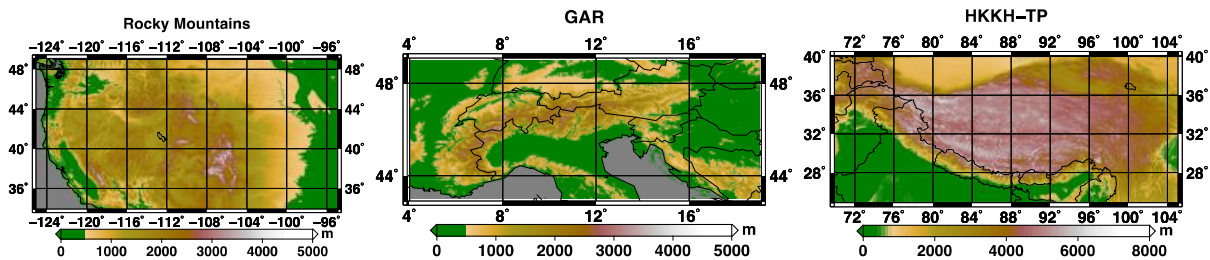


Figure 2. Topographic maps of the three study areas (left: Rocky Mountains; middle: Greater Alpine Region; right: Hindu Kush–Karakoram–Himalaya–Tibetan Plateau) from a high-resolution Digital Elevation Model at 0.0167° resolution. Green areas lie below 500 m a.s.l. and are excluded in our analysis (Palazzi et al., 2018)

The first step to assess EDW is to quantify a warming signal. In this study, this is evaluated as the difference between the 2039–2068 future climatology and the 1979–2008 past climatology of the minimum and of the maximum daily temperature (Δt_{asmin} , Δt_{asmax}). The temperature change between the future and past climatology is evaluated on a seasonal basis using the standard definition of the seasons for the Northern Hemisphere mid-latitudes: winter (December–February, DJF), spring (March– May, MAM), summer (June–August, JJA), and autumn (September–November, SON).

The second step is to assess whether the warming signal in minimum and maximum temperatures exhibits a dependence on elevation. As commonly done in the literature (e.g. Pepin and Lundquist 2008; Liu et al. 2009; Qin et al. 2009; Rangwala et al. 2010, 2012; Palazzi et al. 2017), we calculate the slope obtained by linear regression of timeseries of daily minimum or maximum temperature against the model elevation and we assess its statistical significance. The regression is performed both at each grid point and using data averaged into elevational bands. The statistical significance of the linear slopes is assessed using a *Student's t test*, which tests against the null hypothesis that the coefficient of the regression is zero (no slope). We also explore a methodology based on grouping the temperature change data into elevation bins and then fitting the Probability Density Function (PDF) of the temperature changes evaluated for each bin with a LOcal regrESSion (LOESS) method. In fact, the uneven distribution of points at different elevations may have an impact on the slope evaluation and the dependence of the temperature changes with

elevation may not be linear. Using the PDF solves the first issue while the LOESS regression would highlight possible departures from linearity. Only grid cells with elevation above 500 m a.s.l. are considered in order to reduce some of the influence of the coastal areas or of other areas generating potential interference, such as the Po Valley in the Greater Alpine Region.

Figures 3 and 4 show, for the minimum and maximum temperature respectively and for the GAR, in black the regression line evaluated using all data, in green the regression line evaluated fitting the average of the data (green dots) in each 100 m-thick elevational bin, and in blue a LOESS fitting curve. Purple shading indicates the probability density of a given minimum temperature change in each elevation bin.

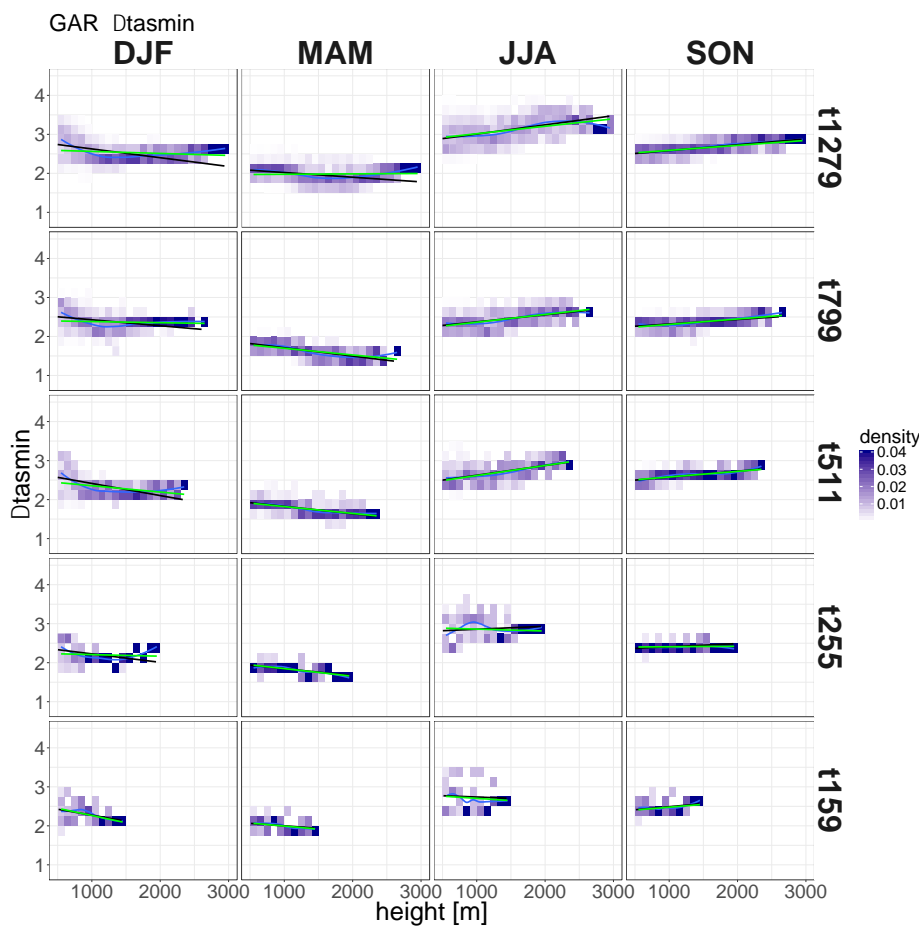


Figure 3. Dependence of minimum daily temperature (*tasmin*) on elevation for the Greater Alpine Region. The black line is the regression line evaluated using all data while the green line that evaluated fitting the average of the data (green dots) into each elevational bin. Superimposed is the PDFs of the temperature change calculated for each bin (shading). The LOESS curved fitting line is also shown in blue. From Palazzi et al., 2018 (supplementary material)

Figure 5 shows, for each model resolution (displayed along the x-axis) and season (each column plot), the value of the slope describing the linear relationship between either the minimum or maximum temperature change and the elevation (corresponding to the slope of the green line in Figs. 3 and 4). Each grey circle indicates the output of one individual model member at each resolution, while the black circle denotes the multi-member mean.

Empty symbols indicate elevational gradients of surface warming that are not statistically significant. Positive slopes in Fig. 5 indicate EDW, while negative slopes highlight the situations in which there is still warming but it is larger at lower elevations (assuming a linear relationship) and we do not focus on this kind of occurrences. Finally, Table 1 summarizes the information provided in Fig. 5.

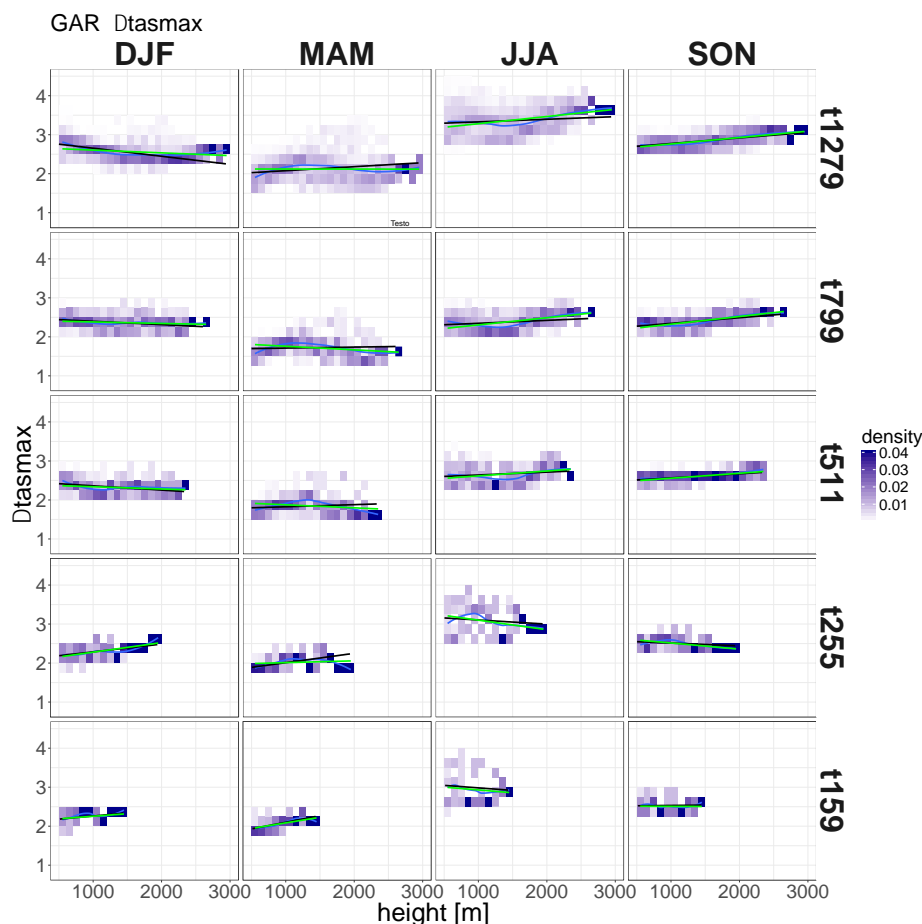


Figure 4. The same as Figure 3, for the maximum temperature (*tasmax*). From Palazzi et al., 2018 (supplementary material)

In the Greater Alpine Region, EDW is detected in summer and autumn at the three finest resolutions, while in winter and spring it is detected only at the coarsest resolutions (T255 and T159 in winter, T159 in spring). The relationship between warming rates and elevation is well represented by a linear model, as clearly visible in Figs. 3 and 4. Further, the PDF of the temperature change in each bin is well peaked around its mean value, which allows to have an unambiguous estimate of the warming expected at each elevation.

The season showing the most striking evidence of EDW in both *tasmin* and *tasmax* is autumn (this is true also for the Rocky Mountains and the Himalayas, which are not discussed in this report, see Palazzi et al., 2018 for details). In fact, the elevational gradients of warming rates in SON exhibit always a positive and statistically significant slope, except for *tasmax* at t255 and t159 resolutions, and the spread among the individual model realizations at each resolution is overall smaller than in the other seasons. EDW is not simulated for *tasmin* in DJF and in MAM: the statistically significant slopes which we found, in fact, are all negative. In some cases, we find considerable variability of the

response among the ensemble members at a given resolution and, in a few cases, some members present both positive and negative slopes. We do not find any clear signal in the response of the different members run in this set of simulations to be directly ascribable to the two possible models used in SPHINX (i.e., the use of either base physics or stochastic parameterizations). This is visible in Fig. 5 looking at the highest resolution (t1279) results, as the only two members available at this resolution, run either with or without stochastic parameterizations, do not provide significantly different EDW response.

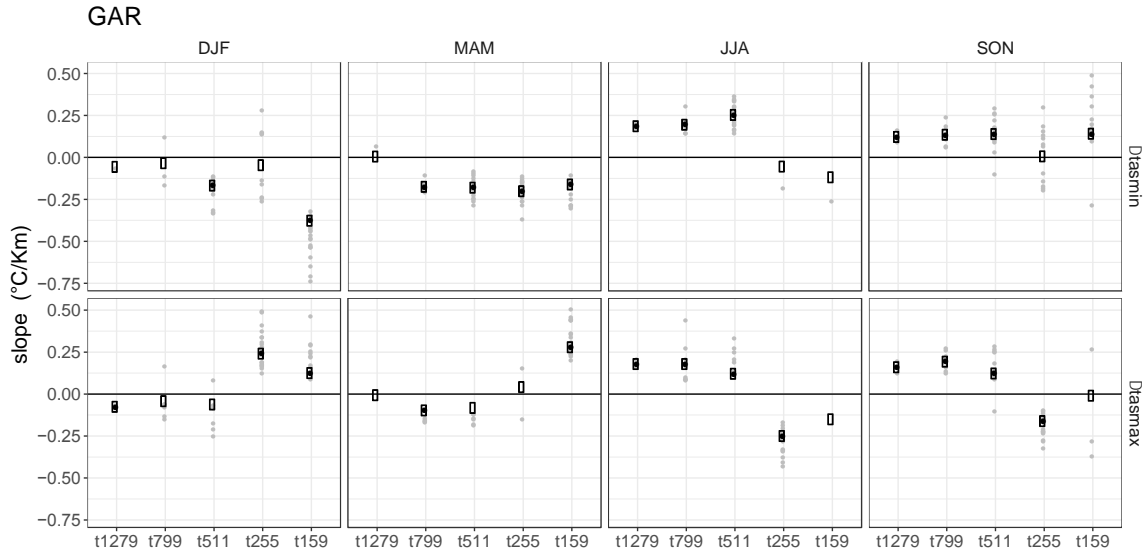


Figure 5. Elevational gradients of the seasonal temperature change in the Greater Alpine Region, for each ensemble member at different EC-Earth model resolutions. The minimum and maximum temperature changes are shown in the top and bottom panels, respectively, while different seasons are organized in the different columns. Each gray circle is the output of one individual model ensemble member at each resolution, while the black circle denotes the multi-member mean. The open symbols represent statistically non-significant elevational gradients of warming rates. From Palazzi et al., 2018.

Table 1. Cases where EDW (i.e., enhanced warming rates with elevation) is detected or not detected (indicated by Y and N respectively). Parentheses indicate cases where the signal is not statistically significant

	<i>tasmin</i>					<i>tasmax</i>				
	t1279	t799	t511	t255	t159	t1279	t799	t511	t255	t159
DJF	(N)	(N)	N	(N)	N	N	(N)	(N)	Y	Y
MAM	(Y)	N	N	N	N	(N)	N	(N)	(Y)	Y
JJA	Y	Y	Y	(N)	(N)	Y	Y	Y	N	(N)
SON	Y	Y	Y	(Y)	Y	Y	Y	Y	N	(N)

In order to identify the variables that may potentially contribute to EDW in the Greater Alpine Region we considered the factors whose changes may alter the surface energy balance and cause temperature variations, including *surface albedo*, *surface downwelling longwave (thermal) and shortwave radiation*, and *near-surface specific humidity*, as already suggested by the literature (e.g. Rangwala and Miller 2012; Palazzi et al. 2017). We calculated the change between the average in the period 2039–2068 and the average in

the period 1979–2008 of the possible EDW drivers (as done for the temperatures) and, in particular, the absolute change for *albedo* ($\Delta albedo$) and the fractional (or normalized) change for *rlds*, *rsds*, and *huss* ($\Delta rlds/rlds0$, $\Delta rsds/rsds0$, $\Delta huss/huss0$). Fractional changes are calculated relative to the averaged climatology between the mean in the years 1979–2008 and the mean in the years 2039–2068). In order for the variables listed above - $\Delta albedo$, $\Delta rlds/rlds0$, $\Delta rsds/rsds0$, $\Delta huss/huss0$ - to be actual EDW drivers, the following conditions have to be satisfied:

- 1) they have to exhibit a dependence on the elevation and the sign of that dependence has to be physically consistent with enhanced warming with elevation, and
- 2) they have to spatially correlate with temperature variations even if the dependence on elevation is removed.

Condition (1) implies that the changes in radiations (*rsds*, *rlds*) and in *huss* have to exhibit the same elevational dependence as the temperature change does: if these variables increase (decrease) also the temperature change increases (decreases). On the contrary, changes in albedo have to exhibit an elevational gradient of opposite sign, since an increase in albedo leads to a reduction of absorbed radiation at the surface and, therefore, to a decrease in surface warming. Basically, condition (1) ensures that the variation with altitude of a given variable and the altitudinal dependence of temperature changes are related with each other by some physical mechanisms. Condition (2) is essential to identify those variables which still (spatially) correlate with temperature changes independently of elevation.

To disentangle the relative importance of the identified EDW drivers in each season and region we set up a multiple linear regression model (see Eq. 1) in which the change in daily minimum or maximum temperature is the predictand and the possible drivers are the predictors. Predictors and the predictand are altitude-detrended, by removing the linear fit on elevation, and standardized, by dividing each change by its standard deviation over the whole spatial domain.

$$\Delta(tasmin, tasmax) = a_1 driver_1 + a_2 driver_2 + \dots + a_n driver_n + \eta \quad (1)$$

In Eq. 1 the drivers correspond to the variables that, among $\Delta albedo$, $\Delta rlds/rlds0$, $\Delta rsds/rsds0$, and $\Delta huss/huss0$, fulfil conditions (1) and (2) listed above. This approach allows to test all the possible combinations of the n predictors that lead to a different regression model. Overall, the possible regression models are $(2^n - 1)$ and their ability in predicting the temperature change is quantified by the coefficient of determination R^2 that measures the proportion of the variance of the predictand that they can explain: the closer R^2 is to 1, the better the prediction is. At the same time, the value of R^2 allows to quantify how much of the EDW response in the model is not explained by the predictors considered. By construction, the regression models including a larger number of predictors are associated with higher values of R^2 . Therefore, to measure the relative quality of the regression models we use the Akaike information criterion corrected for finite sample sizes (AICc), which favors the models with less predictors and penalizes those with more (the lower the AICc, the better the model).

We analyse the role of the four variables, possible drivers of EDW ($\Delta albedo$, $\Delta rlds/rlds0$, $\Delta rsds/rsds0$, $\Delta huss/huss0$) in the GAR, in the different seasons and assessing whether model simulations performed at different spatial resolutions present different behaviours.

From a practical point of view we proceed with the calculation of the three linear Pearson correlation coefficients described below, useful to check if the conditions (1) and (2) are fulfilled:

- R1, between either $\Delta tasmin$ or $\Delta tasmax$ and elevation, and its statistical significance, to highlight the cases with or without EDW.
- R2, between each of the four possible EDW drivers and elevation, and its statistical significance;
- R3, between the (minimum, maximum) temperature change and each of the four possible EDW drivers, and its statistical significance. R3 is calculated after having removed the dependence on elevation of each variable, which is obtained by considering the residuals compared to a linear fit respect to elevation.

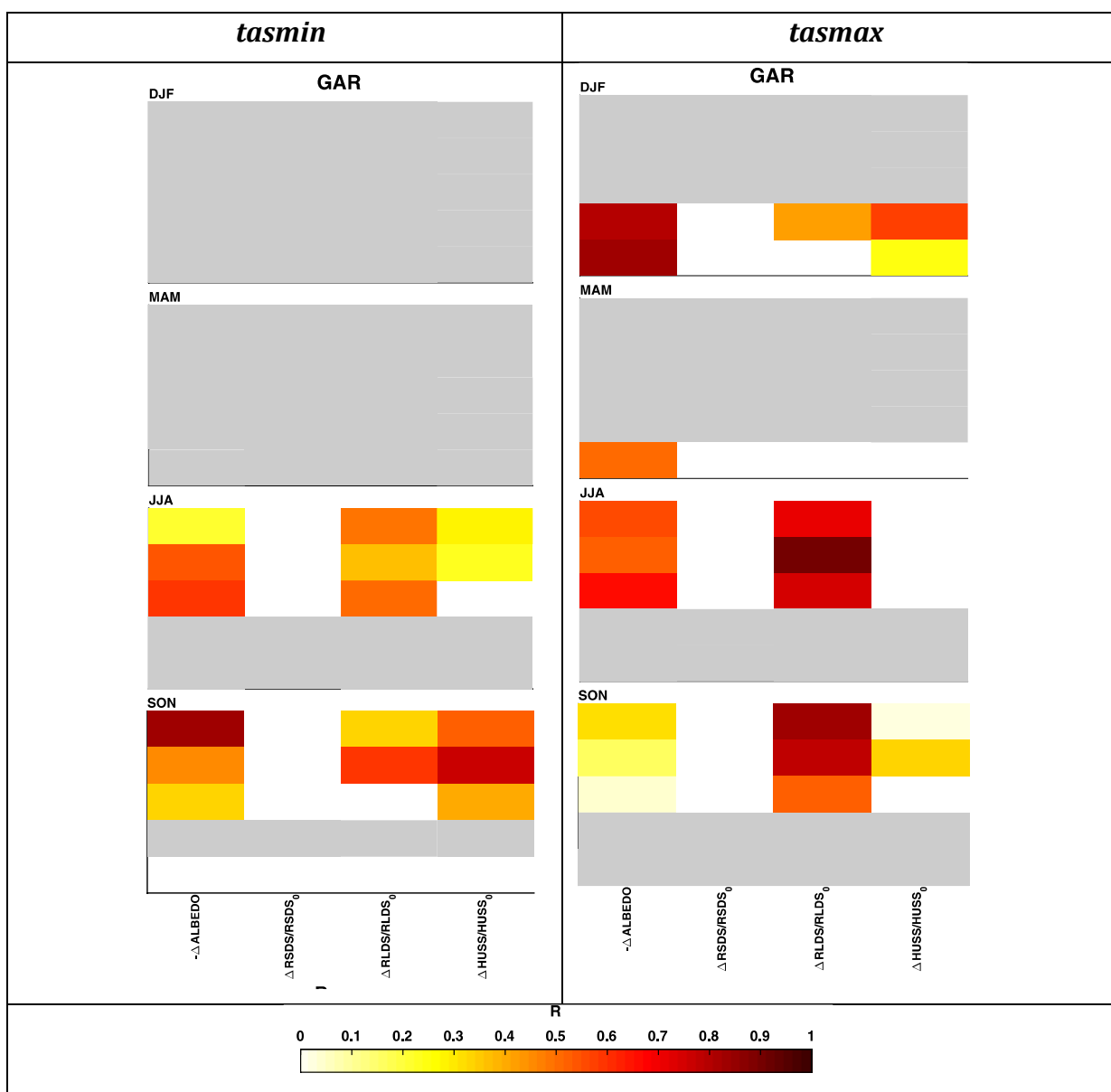


Figure 6. Correlation coefficient between each of the seven possible EDW drivers and the minimum temperature change on the left and the maximum temperature change on the right) in the four seasons. The drivers are displayed along the x-axis. Grey boxes indicate the cases in which there is no EDW or it is not statistically significant. White boxes identify the cases in which R2 is negative or not

statistically-significant and the spatial correlation between a possible driver of EDW and the temperature change is negative. Modified from Palazzi et al., 2018.

A positive sign of R2 for $\Delta rlds/rlds0$, $\Delta rsds/rsds0$, $\Delta huss/huss0$ and $-\Delta albedo$ is physically consistent with EDW (i.e., with the condition $R1 > 0$). Therefore, having R2 greater than zero and statistically significant is one necessary condition for those variables to be actually drivers of EDW. For the variables that fulfil this condition we compute the correlation coefficient R3, measuring their spatial correlation with the temperature change, after having detrended all variables for elevation. The R3 values are shown in Fig. 6 for *tasmin* (left column) and *tasmax* (right column). Grey boxes indicate the cases in which there is no EDW or it is not statistically significant, based on the values of R1, while white boxes identify the situations in which

- for a given variable, R2 is negative or not statistically-significant, which indicates that the variable certainly cannot be a driver of EDW. We recall that the condition $R2 < 0$ applies also to the change in albedo since we use $-\Delta albedo$ in the calculations,

- the spatial correlation between a possible driver of EDW and the temperature change is negative.

Figure 6 thus indicates what are the possible drivers of future EDW in the GAR and how much they correlate (value of R3) with the change in the minimum and maximum temperature. The relative contribution to EDW of the different drivers can be assessed using the multiple linear regression model described by Eq. 1. Since we notice that the season showing the strongest evidence of EDW is SON, for simplicity in the following we discuss in detail the results of application of the multiple linear regression model for SON only. The other seasons are described in a more qualitative way instead. In the GAR, the three drivers of the changes in *tasmin* in JJA and SON (in DJF and MAM EC-Earth did not show EDW) are $\Delta albedo$, $\Delta rlds/rlds0$, and $\Delta huss/huss0$. The only EC-Earth resolutions which are able to identify the simultaneous contribution of all three drivers are T1279 and T799 and we apply the multiple linear regression model only for these two resolutions (and for SON). The results are summarized in Table 2, left columns. At T1279, the four models including $\Delta rlds/rlds0$ as a predictor show the highest values of explained variance among the seven regression models. At T799 the first three models and the fifth in the rank include $\Delta rlds/rlds0$, the model combining $\Delta albedo$ and $\Delta huss/huss0$ ranking fourth. At both resolutions, among the three single-predictor models, the one with $\Delta rlds/rlds0$ shows the highest R2. The three multi-predictor models including $\Delta rlds/rlds0$ in conjunction with any other driver are capable of accounting for more than half the variance of the predictand at T799 (more than 20% at T1279). **Therefore, $\Delta rlds/rlds0$ is found, among the drivers which we considered, essential to drive the changes in *tasmin* in SON in the GAR.**

As for the changes in *tasmax*, we identify as drivers in DJF $\Delta albedo$, $\Delta rlds/rlds0$, and $\Delta huss/huss0$ at T255 and $\Delta albedo$ and $\Delta huss/huss0$ at T159. In JJA, the drivers are $\Delta albedo$ and $\Delta rlds/rlds0$ and the signal is robust across all EC-Earth resolutions (T1279, T799, T511) at which EDW is found. In SON, the drivers are $\Delta albedo$ and $\Delta rlds/rlds0$ at T511 and $\Delta albedo$, $\Delta rlds/rlds0$ and $\Delta huss/huss0$ at T1279 and T799. For the latter two resolutions we discuss the results of application of the multiple linear regression model to study the relative contribution of the three identified drivers (see the right columns in Table 2). $\Delta huss/huss0$ emerges as the most important driver at T1279, while $\Delta albedo$ is the most important driver at T799. In both cases the proportion of the maximum variance explained by the best-performing regression model is quite low (44% at T1279 and 41% at T799).

In general, our analysis shows that the more frequent EDW drivers in all seasons are the changes in albedo and in downward thermal radiation and this is reflected in both daytime and nighttime warming. It is clear that our picture omits other factors which may contribute to EDW in the different regions. It is interesting to observe that in the Alps, and at the coarsest horizontal resolutions only, a significant EDW signal related to albedo changes is observed in the DJF season. At the coarsest resolutions, the orography is smooth, and the highest elevations are not realistically represented in the climate model. This result seems to suggest that the “model’s highest elevations” might undergo an earlier (winter) transition from being snow covered to being snow free in the future in winter months. Of course this signal is an artifact typical of the coarsest resolutions and disappears at finer resolutions when the orography is represented with more accuracy. On the contrary, the finest resolutions are the only ones able to catch the change in albedo as an EDW driver in SON in the GAR. This result would suggest an added value of the finest resolution simulations in the Alpine area.

Table 2. Application of the Eq. 1 including the three predictors ($\Delta albedo$, $\Delta huss/huss_0$ and $\Delta rlds/rlds_0$) of the minimum (left) and maximum (right) temperature change in the GAR in SON. For each of the seven regression models obtained from the combination of the three predictors, the table shows the values of the regression coefficients a_1 (referring to $\Delta albedo$), a_2 (referring to $\Delta huss/huss_0$) and a_3 (referring to $\Delta rlds/rlds_0$), of the coefficient of determination R^2 and of the AICc. See Palazzi et al., 2018.

GAR, SON											
$\Delta(tasmin, tasmax) = a_1 \Delta albedo + a_2 \Delta huss/huss_0 + a_3 \Delta rlds/rlds_0$											
	Rank	$\Delta tasmin$					$\Delta tasmax$				
		$\Delta albedo$	$\frac{\Delta huss}{huss_0}$	$\frac{\Delta rlds}{rlds_0}$	R^2	AICc	$\Delta albedo$	$\frac{\Delta huss}{huss_0}$	$\frac{\Delta rlds}{rlds_0}$	R^2	AICc
		a_1	a_2	a_3			a_1	a_2	a_3		
T1279	1	-0.424	-0.170	0.456	0.356	-0.168	-0.511	-0.854	0.340	0.443	-0.361
	2	-0.354	-	0.385	0.339	-0.144	-0.500	-0.672	-	0.359	-0.221
	3	-	0.054	0.442	0.223	0.018	-	-0.584	0.323	0.250	-0.065
	4	-	-	0.470	0.221	0.020	-	-0.417	-	0.174	0.031
	5	-0.409	0.074	-	0.203	0.043	-0.156	-	-	0.024	0.197
	6	-0.447	-	-	0.200	0.047	-0.160	-	-0.017	0.025	0.198
	7	-	0.283	-	0.080	0.186	-	-	0.021	0.001	0.221
T799	1	-0.361	0.144	0.504	0.612	-0.295	-0.538	-0.376	0.546	0.411	-0.256
	2	-0.419	-	0.575	0.601	-0.270	-0.387	-	0.363	0.337	-0.140
	3	-	0.350	0.459	0.516	-0.076	-0.459	-	-	0.210	0.032
	4	-0.304	0.459	-	0.442	0.067	-0.476	-0.035	-	0.211	0.034
	5	-	-	0.658	0.432	0.084	-	-0.068	0.479	0.197	0.052
	6	-	0.610	-	0.373	0.184	-	-	0.440	0.193	0.053
	7	-0.533	-	-	0.284	0.313	-	0.203	-	0.041	0.226

Finally, it is important to stress that enhancing the spatial resolution in climate models may be crucial especially in complex topography, but also improvements in model parameterizations, particularly those involving surface processes in high-mountain areas, the snow-albedo and cloud-radiation feedbacks, may allow for a better simulation of EDW in the models. Considering the importance that mountains have as early warning indicators of the consequences of global warming, EDW is a phenomenon that calls for further research and efforts, both in terms of observations and of model simulations.

Employed Datasets and data availability

Model data

The specific set of simulations with the EC-Earth GCM presented above were performed in the framework of the PRACE project “Climate SPHINX” (Stochastic Physics High resolution eXperiments), whose detailed description can be found in Davini et al. (2017) and in the project web pages (<http://www.to.isac.cnr.it/sphinx/>). Briefly, these are atmosphere-only experiments extending for 30 years in the past (from 1979 to 2008) and 30 years in the future (from 2039 to 2068) using forcing conditions from the Representative Concentration Pathway emission scenario RCP 8.5 (Riahi et al. 2011), which assumes no stabilization in greenhouse gas emissions during the 21st century. For each resolution, more than one model member was produced. However, owing to computational costs, a different number of EC-Earth members is available for each resolution, from twenty (coarsest resolution) down to two (finest resolution). A peculiarity of the SPHINX experiment is that half of the members at each resolution was run including base physics while the other half using stochastic parameterizations (Davini et al. 2017), the latter being a way to include small-scale processes in coarse resolution without being computationally-demanding. These ensembles gave us the opportunity to gauge both the internal variability of the EC-Earth model and the uncertainty associated with the specific model chosen (either as model implement base physics and the model with stochastic parameterizations). The SPHINX dataset can be accessed upon registration here: <http://wilma.to.isac.cnr.it/sphinx/?q=content/data-access>. The processed SPHINX data for the EDW analysis in the Alpine region presented above can be requested sending an email to: e.palazzi@isac.cnr.it.

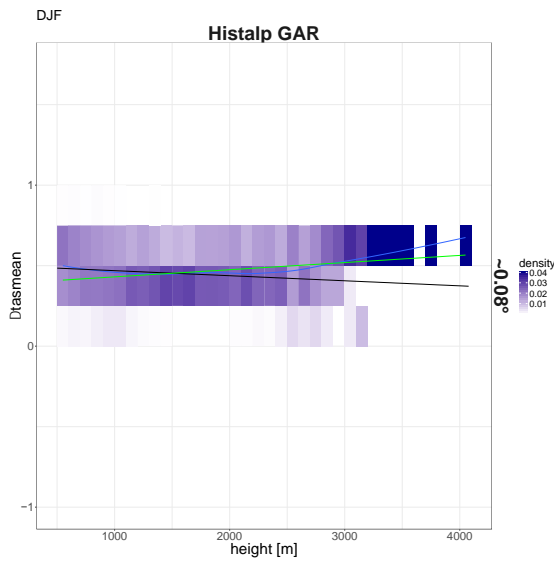
Observation-based data

As already mentioned in the introduction, the lack of a dense and homogeneous network of in-situ stations over mountain areas, especially up to the higher elevations represents a limitation for the analysis and understanding of EDW. This holds true also for the Greater Alpine Region (GAR), though being one of the most instrumented mountain area. The study presented above employs model data to study EDW both because they are more suitable when trying to understand the mechanisms at work and because of the lack of a high-resolution and homogeneous in-situ station network for the entire Alpine chain.

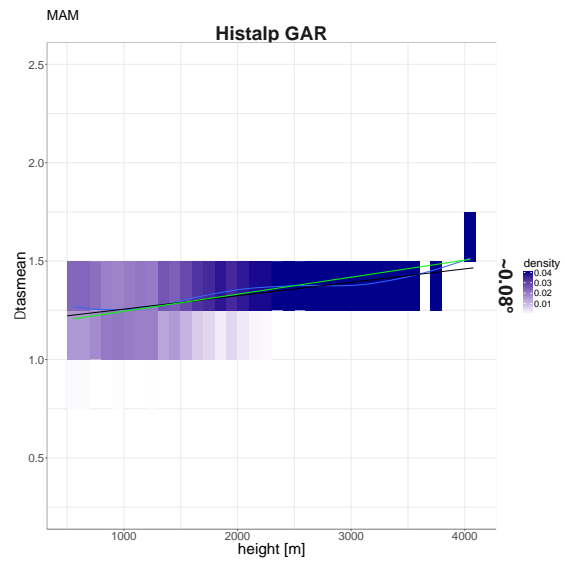
However, we made an exercise also employing an observation-based gridded dataset to assess EDW in the Alps over the past decades, the HISTALP dataset (<http://www.zamg.ac.at/histalp/>). It consists of monthly homogenised temperature, pressure, precipitation, sunshine and cloudiness records for the Greater Alpine Region, with a spatial resolution of about 0.08° latitude-longitude. The longest temperature and air pressure series extend back to 1760, precipitation to 1800, cloudiness to the 1840s and sunshine to the 1880s. We analysed this dataset to assess EDW in the GAR between 1971 and 2015, by calculating, for each season, the change between the mean temperature climatology over the period 1971-1990 and the temperature climatology over the period 1995-2014 and thus proceeding with the EDW assessment as explained above in this Section.

Using the same graphical visualization employed for the analysis of the EC-Earth model data, we summarize the obtained results in Fig 7. Our preliminary results, deserving further investigation in the future, show that EDW is observed in the Alps over the period 1971-2014 only in winter and spring (see the green line in the plots) while surface warming has decreased with elevation in summer and autumn.

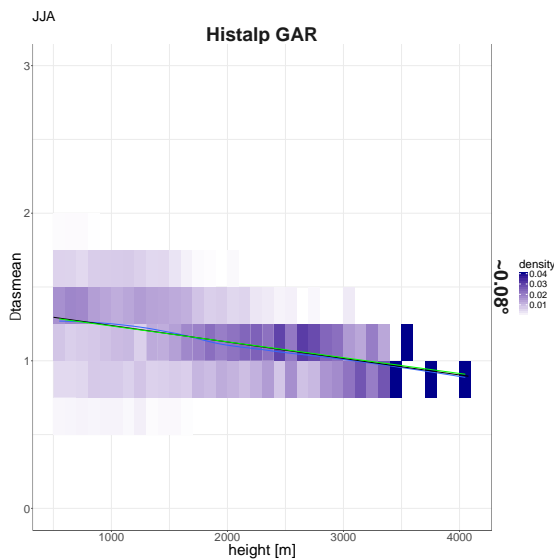
Winter



Spring



Summer



Autumn

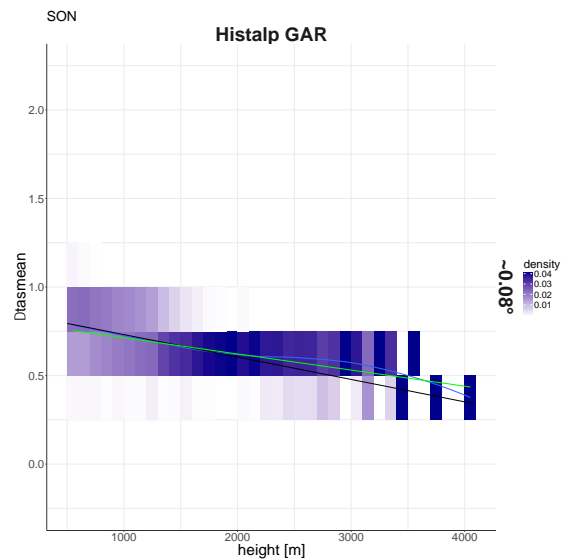


Figure 7. Dependence of mean daily temperature on elevation for the Greater Alpine Region using the HISTALP dataset. The black line is the regression line evaluated using all data while the green line that evaluated fitting the average of the data (green dots) into elevational bins. Superimposed is the PDFs of the temperature change calculated for each bin (shading). The LOESS curved fitting line is also shown in blue.

The processed HISTALP data for the EDW analysis in the Alpine region can be requested sending an email to: e.palazzi@isac.cnr.it.

Rereferences

- Davini P, von Hardenberg J, Corti S, Christensen HM, Juricke S, Sub-ranian A, Watson PAG, Weisheimer A, Palmer TN (2017) Climate SPHINX: evaluating the impact of resolution and stochastic physics parameterisations in the EC-Earth global climate model. *Geosci Model Dev* 10:1383–1402. <https://doi.org/10.5194/gmd-10-1383-2017>

- Demory M-E, Vidale PL, Roberts MJ, Berrisford P, Strachan J, Schiemann R, Mizieliński MS (2014) The role of horizontal resolution in simulating drivers of the global hydrological cycle. *Clim Dyn* 42:2201–2225
- Duan, A., and G. Wu (2006), Change of cloud amount and the climate warming on the Tibetan Plateau, *Geophys. Res. Lett.*, 33, L22704, doi:10.1029/2006GL027946.
- Fyfe JC, Flato JM (1999) Enhanced climate change and its detection over the Rocky Mountains. *J Clim* 12:230–243. <https://doi.org/10.1175/1520-0442-12.1.230>
- Hazeleger W, Severijns C, Semmler T, Ștefănescu S, Yang S, Wang X, Wyser K, Dutra E, Baldasano JM, Bintanja R, Bougeault P, Caballero R, Ekman AML, Christensen JH, van den Hurk B, Jimenez P, Jones C, Källberg P, Koenigk T, McGrath R, Miranda P, Van Noije T, Palmer T, Parodi JA, Schmith T, Selten F, Storelvmo T, Sterl A, Tapamo H, Vancoppenolle M, Viterbo P, Willén U (2010) EC-Earth: a seamless earth-system prediction approach in action. *Bull Am Meteorol Soc* 91:1357–1363. <https://doi.org/10.1175/2010BAMS2877.1>
- Hazeleger W, Wang X, Severijns C, Ștefănescu S, Bintanja R, Sterl A, Wyser K, Semmler T, Yang S, van den Hurk B, van Noije T, van der Linden E, van der Wiel K (2012) EC-Earth V2.2: description and validation of a new seamless earth system prediction model. *Clim Dyn* 39:2611–2629. <https://doi.org/10.1007/s00382-011-1228-5>
- IPCC (2013) *Climate Change 2013: The Physical Science Basis*. In: Stocker TF, Qin D, Plattner G-K, Tignor M, Allen SK, Boschung J, Nauels A, Xia Y, Bex V, and Midgley PM (eds.) Contribution of working group I to the fifth assessment report of the intergovernmental panel on climate change. Cambridge University Press, Cambridge
- Liu X, Cheng Z, Yan L, Yin Z-Y (2009) Elevation dependency of recent and future minimum surface air temperature trends in the Tibetan Plateau and its surroundings. *Global Planet Chang* 68:164–174. <https://doi.org/10.1016/j.gloplacha.2009.03.017>
- Palazzi E, Filippi L, von Hardenberg J (2017) Insights into elevation-dependent warming in the Tibetan Plateau–Himalayas from CMIP5 model simulations. *Clim Dyn* 48(11–12):3991–4008. <https://doi.org/10.1007/s00382-016-3316-z>
- Palazzi, E., Mortarini, L., Terzago, S. et al. *Clim Dyn* (2018). <https://doi.org/10.1007/s00382-018-4287-z>
- Pepin, N., Bradley, R.S., Diaz, H.F., Baraer, M., Caceres, E.B., Forsythe, N., Fowler, H., Greenwood, G., Hashmi, M.Z., Liu, X.D., Miller, J.R., Ning, L., Ohmura, A., Palazzi, E., Rangwala, I., Schöner, W., Severskiy, I., Shahgedanova, M., Wang, M.B., Williamson, S.N., Yang, D.Q., Elevation-dependent warming in mountain regions of the world (2015) *Nature Climate Change*, 5 (5), pp. 424-430. DOI: 10.1038/nclimate2563, 2015.
- Pepin NC, Lundquist JD (2008) Temperature trends at high elevations: patterns across the globe. *Geophys Res Lett* 35:L14701. <https://doi.org/10.1029/2008GL034026>
- Qin J, Yang K, Liang S, Guo X (2009) The altitudinal dependence of recent rapid warming over the Tibetan Plateau. *Clim Chang* 97:321–327. <https://doi.org/10.1007/s10584-009-9733-9>
- Ramanathan, V. and G. Carmichael (2008), Global and regional climate changes due to black carbon, *Nature Geoscience* volume 1, pages 221–227
- Rangwala I, Miller JR, Russell GL, Xu M (2010) Using a global climate model to evaluate the influences of water vapor, snow cover and atmospheric aerosol on warming in the Tibetan Plateau during the twenty-first century. *Clim Dyn* 34:859–872. <https://doi.org/10.1007/s00382-009-0564-1>
- Rangwala I, Barsugli J, Cozzetto K, Neff J, Prairie J (2012) Mid-21st century projections in temperature extremes in the southern Colorado Rocky Mountains from regional climate models. *Clim Dyn* 39:1823–1840. <https://doi.org/10.1007/s00382-011-1282-z>
- Rangwala I, Miller JR (2012) Climate change in mountains: a review of elevation-dependent warming and its possible causes. *Clim Chang* 114:527–547. <https://doi.org/10.1007/s10584-012-0419-3>
- Rangwala I, Sinsky E, Miller RJ (2013) Amplified warming projections for high altitude regions of the Northern hemisphere mid-latitudes from CMIP5 models. *Environ Res Lett* 8:024040. <https://doi.org/10.1088/1748-9326/8/2/024040>

- Rangwala I, Sinsky E, Miller RJ (2016) Variability in projected elevation dependent warming in boreal midlatitude winter in CMIP5 climate models and its potential drivers. *Clim Dyn* 46(7):2115–2122. <https://doi.org/10.1007/s00382-015-2692-0>
- Riahi K, Rao S, Krey V, Cho C, Chirkov V, Fischer G, Kindermann G, Nakicenovic N, Rafaj P (2011) RCP 8.5—a scenario of comparatively high greenhouse gas emissions. *Clim Chang* 109:33–57, <https://doi.org/10.1007/s10584-011-0149-y>
- Yan L, Liu Z, Chen G, Kutzbach JE, Liu X (2016) Mechanisms of elevation-dependent warming over the Tibetan plateau in quadrupled CO₂ experiments. *Clim Chang* 135:509–519. <https://doi.org/10.1007/s10584-016-1599-z>